

A deterministic photon free method to solve radiation transfer equations

Britton Chang *

*Center for Applied Scientific Computing, Lawrence Livermore National Laboratory, P.O. Box 808, L-561,
Livermore, CA 94551, United States*

Received 8 September 2005; received in revised form 31 May 2006; accepted 22 June 2006
Available online 31 October 2006

Abstract

A new method to solve radiation transfer equations is presented. In the absence of scattering, material motion, and heat conduction, the photon variables can be eliminated from the fully implicit, multi-group, discrete-ordinate, finite difference (finite element) equations of continuum radiation transfer to yield a smaller set of equations which depends only on temperature. The solution to this smaller set of equations is used to generate the solution to the original set of equations from which the reduced set is derived. The reduced system simplifies to a nonlinear heat equation in the regime of strong absorption and strong emission. We solve the reduced set of equations by the Newton-GMRES method in which the Jacobian update is preconditioned by a linearization of this nonlinear heat equation. The performances of this new method and of the semi-implicit linear method, which is preconditioned by grey transport acceleration combined with diffusion synthetic acceleration, are compared on two test problems. The test results indicate that the new method can take larger time steps, requires less memory, is more accurate, and is competitive in speed with the semi-implicit linear method.

© 2006 Elsevier Inc. All rights reserved.

Keywords: Radiation transport; Nonlinear systems; Newton-GMRES

1. Introduction

Conventional deterministic methods [3,18,26,28] for radiative transfer simulations solve not the nonlinear equations of continuum radiative transfer, but solve the semi-implicit linear approximation (SiL) [18] of these equations. Since the linear equations of the SiL approximation merge into the nonlinear equations of radiative transfer as the time step is decreased, simulations by conventional methods are accurate for small time increments. However, for larger time steps, as we shall see, the SiL approximation may yield solutions which are outside of the bounds permitted by the nonlinear equations; these bounds were derived by Amdreev et al. [5]. This unphysical behavior of the SiL approximation is unexpected, since the time derivatives of its equations are implicitly differenced. Furthermore, since this unphysical behavior was proved by Amdreev et al. [5] to be absent in the solutions of the implicitly differenced, multi-group, discrete-ordinate, finite difference nonlinear

* Tel.: +1 925 423 6416; fax: +1 925 423 2993.
E-mail address: bchang@llnl.gov.

equations of radiative transfer, the goal of this paper is to demonstrate that these equations can be solved without the simplifying assumptions of the SiL approximation.

We solve this discrete system with Newton's method [16], not by plugging it as is into Newton's method, since its sheer size is daunting, but by deriving from it a smaller but equivalent set of equations which is then plugged into Newton's method. The equations of continuum radiation transfer consist of two coupled sub-systems: a transport equation for the intensity ψ , and a material equation for the temperature T . Hence, the number of unknowns in a discretization of these equations is of the order of $n_g \times n_d \times n_x$, where n_g is the number of groups, n_d is the number of directions, and n_x is the number of zones. As we shall see, this coupled system can be trimmed down to a manageable size by eliminating the intensity from the system, leaving behind a material-like equation for the temperature, which is then solved by Newton's method. Since the material-like equation consists of n_x unknowns, Newton's method can solve this reduced system more efficiently than the underlying system from which the reduced system is derived. This idea of deriving a reduced system is borrowed from the symbolic implicit Monte-Carlo (SIMC) method [7,25,27], but, unlike the SIMC method, our method is deterministic.

There is a potential roadblock in Newton's method; it requires the inversion of a non-symmetric matrix known as the Jacobian. We clear this barrier for iterative inversion methods by deriving in Section 3 a preconditioner for the Jacobian from the large cross section limit of the material-like temperature equation. In this limit, the material-like equation simplifies to a nonlinear heat equation, which when linearized yields a preconditioner. Results presented in Section 4 on the inversion of the Jacobian by the GMRES method [30] show the accelerating effect of this preconditioner.

A reduced system is also derived by the SiL approximation. Unlike our approach, the SiL approximation eliminates the temperature from the coupled sub-systems to yield a transport-like equation for the intensity. However, this approach, as shown in Section 5, requires two approximations: the coefficients of the sub-systems are frozen within a time step, and the black body emission function is approximated. Both approximations¹ are also employed to eliminate the temperature from the coupled subsystems by the implicit Monte-Carlo (IMC) [14] method. The unphysical behavior of the SiL approximation for large time steps discussed above was also observed by Larsen and Mercier [19] in the IMC results for large time steps. On the other hand, the elimination of the photon variables from the sub-systems requires no approximation beyond discretization. The reason, which will become clearer in Section 2, is because we can solve the photon equation, an equation which is linear in ψ but is nonlinear in T , for the intensity in the usual way with a sweeping operator whose coefficients are nonlinear functions of temperature. We can then substitute the result into the material equation to yield an equation that depends solely on temperature. As we shall see in the test results of Section 4, the absence of these two approximations enables our method to take time steps that are considerably larger than the time steps that the SiL method can take stably.

2. The multi-group and the discrete-ordinate approximation for radiative transfer

For clarity of exposition, we restrict our discussion to slab geometry and local thermodynamic equilibrium. In the absence of scattering, material motion, and heat conduction, the multi-group, discrete-ordinate equations of radiative transfer, Section VII.C of [2], consist of the transport equation,

$$\frac{1}{c} \frac{\partial \psi_{g,d}}{\partial t} + \mu_d \frac{\partial \psi_{g,d}}{\partial x} + \sigma_g(T) \psi_{g,d} = \sigma_g(T) B_g(T) + s_{g,d}, \quad \begin{array}{l} g = 1, \dots, n_g, \\ d = 1, \dots, n_d, \end{array}$$

and the material equation,

$$C_p(T) \frac{\partial T}{\partial t} = \sum_{g=1}^{n_g} \sum_{d=1}^{n_d} \sigma_g(T) w_d (\psi_{g,d} - B_g(T)) + q,$$

where

$$B_g(T) = \int_{\nu_{g-\frac{1}{2}}}^{\nu_{g+\frac{1}{2}}} \frac{4\pi h \nu^3}{c^2} \frac{e^{-h\nu/kT}}{1 - e^{-h\nu/kT}} d\nu, \quad (2.1)$$

¹ The approximation of the black body emission function is of $O(\Delta T)$ in the IMC method but is of $O((\Delta T)^2)$ in the SiL approximation.

is the group integrated² Planck function,

$$C_p(T) = \rho(T)C_v(T),$$

is the product of the mass density $\rho(T)$ and the heat capacity at constant volume $C_v(T)$, and $\{w_d\}$ is the set of quadrature weights that sums to 2. In these equations, c is the speed of light, h is Planck’s constant, k is Boltzmann’s constant, g is the group index, d is the direction index, $\sigma_g(T)$ is the group averaged cross section, $s_{g,d}$ is a frequency and direction dependent external radiation source, and q is an external heat source.

If the system is discretized by the backward Euler Method, and if the superscript n represents the beginning of a time step and the absence of a superscript represents the end of a time step, we have

$$\begin{aligned} \mu_d \frac{\partial \psi_{g,d}}{\partial x} + \left(\sigma_g(T) + \frac{1}{c\Delta t_n} \right) \psi_{g,d} &= \sigma_g(T)B_g(T) + s_{g,d} + \frac{\psi_{g,d}^n}{c\Delta t_n}, \\ C_p(T) \frac{T - T^n}{\Delta t_n} &= \sum_{g=1}^{n_g} \sum_{d=1}^{n_d} \sigma_g(T)w_d(\psi_{g,d} - B_g(T)) + q. \end{aligned}$$

The streaming operator can be discretized by many finite element or finite difference techniques, e.g. the Petrov–Galerkin method [15], the Diamond Difference method [11], the Discontinuous Galerkin method [29], the Corner Balance method [1], the Linear Discontinuous method [17], the Weighted Diamond Difference method [6], etc. As a result of the discretization, the spatial derivative can be expressed as a matrix, which we denote as D , and the boundary conditions can be expressed as a source term, which we denote as $b_{g,d}$. Each discretization, however, lays out ψ on a mesh in its own way. For some discretizations, ψ is node centered, for others, ψ is zone centered and face centered, and for a few, ψ is both. For the sake of clarity, let the discretization of the spatial derivative be zone centered. Although such a discretization is highly inaccurate and is highly unlikely to be used in a simulation, this choice simplifies our presentation. Assuming that $\psi_{g,d}, T$, the external sources, and the boundary condition $b_{g,d}$ are zone centered arrays, that D is a matrix that operates on zone centered arrays, and that $\sigma_g(T)$ and $C_p(T)$ are from here on diagonal matrices whose entries are nonlinear functions of T , the discrete system of nonlinear equations can be written as:

$$\begin{aligned} (\mu_d D + \sigma_g(T) + (c\Delta t_n)^{-1}I)\psi_{g,d} &= \sigma_g(T)B_g(T) + s_{g,d} + (c\Delta t_n)^{-1}\psi_{g,d}^n + b_{g,d}, \\ C_p(T) \frac{T - T^n}{\Delta t_n} &= \sum_{g=1}^{n_g} \sum_{d=1}^{n_d} \sigma_g(T)w_d(\psi_{g,d} - B_g(T)) + q. \end{aligned} \tag{2.2}$$

Let us introduce notation for solving system (2.2). If we define the nonlinear function $\mathcal{G}(\psi, T)$ as the left-hand side (l.h.s.) of (2.2) minus the right-hand side (r.h.s.) of (2.2), then system (2.2) can be written as $\mathcal{G}(\psi, T) = 0$. We define the solution of (2.2) as the set of $\psi_{g,d}$ ’s and the T , which when substituted into $\mathcal{G}(\psi, T)$ yields 0. If an arbitrary set of $\psi_{g,d}$ ’s and an arbitrary T are substituted into $\mathcal{G}(\psi, T)$ we define the non-zero result as the nonlinear residual. Thus, the solution of (2.2) is the set of $\psi_{g,d}$ ’s and the T which yield a zero nonlinear residual. The goal of an iterative method is to reduce the nonlinear residual $\mathcal{G}(\psi, T)$ with each iteration.

There are two main strategies for reducing the nonlinear residual $\mathcal{G}(\psi, T)$. The first, taken by conventional deterministic methods [3,18,26,28], is to linearize system (2.2), and then eliminate the temperature from the linearized system to give a transport equation with an additional scattering term. The other strategy for reducing the nonlinear residual is to solve the first equation of (2.2) for the intensity and then substitute the intensity into the material equation. This approach is taken by the SIMC method. It is also the approach that would be taken by a linear algebraist, if (2.2) were a linear system. A linear algebraist would solve the first equation of (2.2) for the intensity, and then substitute the intensity into the second equation of (2.2), leaving behind the Schur Complement [30] of (2.2).

The matrix of the l.h.s. of the first equation of (2.2) is easy to invert, because *it does not have scattering*. If we define that matrix as

$$H_{g,d}(T) \equiv \mu_d D + \sigma_g(T) + (c\Delta t_n)^{-1}I, \tag{2.3}$$

² Normalization of $B_v(T) : \int_0^\infty dv \int_{-1}^1 d\mu \frac{4\pi h\nu^3}{c^2} \frac{e^{-h\nu/kT}}{1 - e^{-h\nu/kT}} = \frac{8\pi^2 k^4 T^4}{15h^3 c^2}$.

define the last three terms on the r.h.s. of the first equation of (2.2) as

$$f_{g,d}^n \equiv s_{g,d} + (c\Delta t_n)^{-1}\psi_{g,d}^n + b_{g,d},$$

substitute the solution of the first equation of (2.2) into the second equation of (2.2), and multiply the result by Δt_n , then we have the discrete analog of the SIMC temperature equation,

$$C_p(T)(T - T^n) = \sum_{g,d=1}^{n_g, n_d} \Delta t_n \sigma_g(T) w_d (H_{g,d}^{-1}(\sigma_g(T) B_g(T) + f_{g,d}^n) - B_g(T)) + q \Delta t_n. \quad (2.4)$$

The matrix, $H_{g,d}^{-1}$, in (2.4) is known as the sweeping operator in transport theory. The product, $H_{g,d}^{-1} \cdot \sigma_g(T) B_g(T)$, is operationally equivalent to a matrix-vector product.

If we can find the T that solves (2.4), then we also have the solution to the underlying system (2.2). The reason is because if we substitute the T that solves (2.4) into the first equation of (2.2), then we can complete the solution of (2.2) by back-solving the first equation of (2.2) for the intensity $\psi_{g,d}$. Let us introduce notation for solving (2.4). If we define, $\mathcal{F}(T)$, as the nonlinear residual of (2.4),

$$\mathcal{F}(T) \equiv C_p(T)(T - T^n) - \sum_{g,d=1}^{n_g, n_d} \Delta t_n \sigma_g(T) w_d (H_{g,d}^{-1}(\sigma_g(T) B_g(T) + f_{g,d}^n) - B_g(T)) - q \Delta t_n,$$

then (2.4) can be written as:

$$\mathcal{F}(T) = 0. \quad (2.5)$$

Nonlinear solvers for (2.5) require the evaluation of $\mathcal{F}(T)$, which is facilitated by the first equation of (2.2),

$$H_{g,d}(T)\psi_{g,d} = \sigma_g(T)B_g(T) + f_{g,d}^n, \quad (2.6)$$

written in matrix form. For the iterate, T_k , it is straightforward to evaluate the terms $C_p(T_k)$, $\sigma_g(T_k)$, and $B_g(T_k)$ of $\mathcal{F}(T_k)$. The term, $H_{g,d}^{-1}(\sigma_g(T_k)B_g(T_k) + f_{g,d}^n)$, is determined by solving the transport equation, $H_{g,d}(T_k)\psi_{g,d} = \sigma_g(T_k)B_g(T_k) + f_{g,d}^n$.

3. Newton-GMRES method for solving the temperature equation

The Newton-GMRES method for solving (2.5) is Newton's method for systems in which the Jacobian of $\mathcal{F}(T)$ is inverted by the GMRES method [30]. Newton's method starts with an initial guess, T_0 , and finds the next iterate by solving a linear system. Let the subscript k be the index of the current iterate, then the linear system that determines the next iterate in Newton's method is

$$\mathcal{F}(T_k) + \mathbf{J}(T_{k+1} - T_k) = 0,$$

where

$$\mathbf{J} \equiv \left. \frac{\partial \mathcal{F}}{\partial T} \right|_{T_k},$$

is the matrix formed by the partial derivatives of \mathcal{F} evaluated at T_k . Inverting \mathbf{J} by the GMRES method, we have

$$T_{k+1} = T_k - \mathbf{J}^{-1} \mathcal{F}(T_k).$$

The inversion of \mathbf{J} for solving the linear system, $\mathbf{J}x = b$, by the GMRES method requires a function that returns the action of \mathbf{J} on an arbitrary vector z . We provide in Appendix 1 a matrix-free formula for computing $\mathbf{J}z$. However, that matrix-free formula, which requires two sweeps to compute $\mathbf{J}z$ is more expensive than the following forward difference quotient formula³, which requires one⁴ sweep to compute $\mathbf{J}z$,

³ The error in the forward quotient approximation and its effect on the efficiency of Newton's method is discussed in [9] and [16].

⁴ Since $\mathcal{F}(T_k)$ is known from the last iterate and can be stored in memory, the work to evaluate the forward difference formula is a single sweep.

$$\mathbf{Jz} \approx \frac{\mathcal{F}(T_k + \epsilon z) - \mathcal{F}(T_k)}{\epsilon},$$

where ϵ is a small number. Hence, for practical reasons, we compute \mathbf{Jz} by the above approximation.

3.1. Initial guess

Since a nonlinear solver with line searching logic does not require an accurate initial guess to converge [16], we take T_n , the temperature at the beginning of a time step, to be our initial guess. However, since an accurate initial guess may improve the efficiency of the solver, we provide in Appendix 2 an approximate solution for $\mathcal{F}(T) = 0$, which can serve as an initial guess.

3.2. A heat conducting preconditioner

Newton’s method is as effective as its linear preconditioner. If the time step and the cross section are both large, then, as shown below, \mathbf{J} is nearly singular. Furthermore, the condition number of \mathbf{J} grows as the cross section increases. Since an unpreconditioned iterative inversion of a matrix decelerates as the condition number of the matrix increases, then the importance of the preconditioning of \mathbf{J} increases with increasing cross section magnitude. It is easy to derive an effective preconditioner for $\partial\mathcal{F}(T)/\partial T$ in the regime of vanishing cross section, because, by (2.4), $\mathcal{F}(T) \rightarrow C_p(T)(T - T^n) - q\Delta t_n$ in this limit. It is also easy to derive an effective preconditioner in the regime of large cross section, because, in this limit, $\mathcal{F}(T) = 0$ simplifies to a nonlinear heat conduction equation.

Let us derive the large cross section limit of $\mathcal{F}(T) = 0$ from (2.4). When $\sigma_g(T)$ is large, the sweeping operator $H_{g,d}^{-1}$, see (2.3), can be approximated by the three term Neumann series⁵,

$$H_{g,d}^{-1} \equiv (I + \tilde{\sigma}_g^{-1} \mu_d D)^{-1} \tilde{\sigma}_g^{-1} = (I - \tilde{\sigma}_g^{-1} \mu_d D + (\tilde{\sigma}_g^{-1} \mu_d D)^2 + \dots) \tilde{\sigma}_g^{-1},$$

where $\tilde{\sigma}_g \equiv \sigma_g(T) + (c\Delta t_n)^{-1}I$. When this series is substituted into (2.4), the identities, $\sum_{d=1}^{n_d} w_d = 2$, $\sum_{d=1}^{n_d} w_d \mu_d = 0$, and $\sum_{d=1}^{n_d} w_d \mu_d^2 = 2/3$, enable us to collapse the sums with respect to the direction index d in (2.4). The steps to collapse these sums are: right multiply the above series by $\sigma_g(T)$, subtract I from the product, multiply the difference by w_d , and sum the product with respect to d . The result is

$$\sum_{d=1}^{n_d} w_d (H_{g,d}^{-1} \sigma_g(T) - 1) \approx 2\tilde{\sigma}_g^{-1} \left(-\frac{1}{c\Delta t_n} I + D \frac{1}{3\tilde{\sigma}_g} D \tilde{\sigma}_g^{-1} \sigma_g(T) \right).$$

Substituting the above formula into (2.4), we have the nonlinear heat equation

$$C_p(T) \frac{T - T^n}{\Delta t_n} = 2 \sum_{g=1}^{n_g} \sigma_g(T) \tilde{\sigma}_g^{-1} \left(-\frac{1}{c\Delta t_n} I + D \frac{1}{3\tilde{\sigma}_g} D \tilde{\sigma}_g^{-1} \sigma_g(T) \right) B_g(T) + \hat{q}, \tag{3.1}$$

where $\hat{q} = q + \sum_{g,d=1}^{n_g n_d} \sigma_g(T) w_d H_{g,d}^{-1} f_{g,d}^n$. Since (3.1) is the large cross section limit of $\mathcal{F}(T) = 0$, we can derive a preconditioner (at the most current temperature) for $\partial\mathcal{F}(T)/\partial T$ by differentiating (3.1) with respect to T . However, as found in diffusive radiation transport [10,21,23], a preconditioner can be effective even if its coefficients are lagged. To lag $C_p(T)$ and $\sigma_g(T)$ of the preconditioner is to evaluate them at T^n , the temperature at the beginning of the time step. In fact, the preconditioner is updated only once every few time steps in the Newton solvers of some diffusive radiation transport codes [10]. The preconditioner derived from (3.1) is also effective in the thin regime, because (3.1) in this regime merges into the thin limit of $\mathcal{F}(T)$.

The condition number of $\partial\mathcal{F}(T)/\partial T$ for situations of large time steps and large cross sections can be estimated from the T derivative of (3.1) for these conditions. For large Δt_n , the l.h.s. of (3.1) and the first term on the r.h.s. of (3.1) can both be neglected. Furthermore, $\sigma_g(T) \tilde{\sigma}_g^{-1} \approx I$ in (3.1) when Δt_n is large. Differentiating (3.1) with these approximations yields

⁵ We also found that $\tilde{\sigma}_g^{-1}$ the one term Neumann approximation of $H_{g,d}^{-1}$, leads to an effective preconditioner. This idea of approximating $H_{g,d}^{-1}$ with a Neumann series was also used by Larsen et al. [20] to derive the asymptotic approximation of the continuous version of 2.2.

$$\frac{\partial \mathcal{F}(T)}{\partial T} \approx \sum_{g=1}^{n_g} \left(D \frac{1}{3\sigma_g(T)} D \frac{\partial B_g(T)}{\partial T} - D \frac{\frac{\partial \sigma_g(T)}{\partial T}}{3\sigma_g^2(T)} D B_g(T) \right).$$

If $\partial \sigma_g(T) \partial T / \ll \sigma_g^2(T)$ as $\sigma_g(T) \rightarrow \infty$, then $\partial \mathcal{F}(T) / \partial T \rightarrow 0$. Hence, $\partial \mathcal{F}(T) / \partial T$ is ill conditioned for large time steps and large cross sections; an unpreconditioned iterative inversion of $\partial \mathcal{F}(T) / \partial T$ may stall for these conditions.

To complete this section, let us uncover the nonlinear heat equation which is buried in (3.1); it was first derived by Eddington [12] and later solved by Marshak [22]. Assuming the cross section is independent of frequency, the sum with respect to g in (3.1) collapses. This follows because the ratio of cross sections $\sigma_g(T) \tilde{\sigma}_g^{-1} \approx I$ for large cross sections, and the sum of the discrete Planckian over all groups can be approximated by the integral of the continuous Planckian over all frequencies to yield $\sum_g 2B_g(T) \approx acT^4$, where a is the radiation constant, and c is the speed of light. Taking these observations into account, (3.1) reduces to the nonlinear heat equation of Eddington with an additional absorption term

$$C_p(T) \frac{T - T^n}{\Delta t_n} = \left(-\frac{1}{c\Delta t_n} I + D \frac{1}{3\tilde{\sigma}} D \right) acT^4 + \hat{q}.$$

4. Numerical results

The numerical results by the new method, which we call the photon free method (PFM), are compared to the numerical results by the semi-implicit linear (SiL) method [18], which is preconditioned by Grey Transport Acceleration [18] combined with Diffusion Synthetic Acceleration [2,4,8,17,24]. In both methods, the spatial derivative is discretized by the simple corner balance approximation [1]. We compare the robustness, the accuracy, and the speed of the two methods on two test problems. The first is from Larsen's seminal work on Grey Transport Acceleration [18]. The second is from Su's and Olson's work [31] on the solution of a radiation transport problem with a T^3 heat capacity.

The PFM equations are solved with the Livermore's nonlinear solver KINSOL [13], which is a Newton solver with enhancements such as line-searching. A discussion of line searching is beyond the scope of this paper; it is provided however in [16]. We also found that the temperature at the beginning of the time step can be taken to be the initial guess in Newton's method when the line-search option in KINSOL is turned on.

4.1. Larsen's test problem

This test problem is from Larsen's paper on Grey Transport Acceleration [18]. We introduce this problem with a description of the problem's phase space grid. The frequency variable ν is logarithmically spaced with 50 groups between $h\nu_{\min} = 10^{-5}$ keV and $h\nu_{\max} = 10$ keV. Group g is defined by $\nu_{g-\frac{1}{2}} \leq \nu \leq \nu_{g+\frac{1}{2}}$, where

$$\nu_{\frac{1}{2}} = \nu_{\min}, \quad \nu_{g+\frac{1}{2}} = \left(\frac{\nu_{\max}}{\nu_{\min}} \right)^{\frac{1}{50}} \nu_{g-\frac{1}{2}}.$$

The angular quadrature is the 20 point Gauss-Legendre approximation; this set has 5 times more angles than the 4 point Gauss-Legendre set in Larsen's paper. The time steps are constant 30 ps (1 ps = 10^{-12} s) increments. The spatial domain is divided into three regions which is described by the spatial mesh,

$$\Delta x = \begin{cases} .10 \text{ cm}, & 0 < x < 1, \\ .02 \text{ cm}, & 1 < x < 2, \\ .20 \text{ cm}, & 2 < x < 4. \end{cases}$$

We continue the introduction of Larsen's test problem with a description of the problem's physical parameters. The cross section is a model for inverse Bremsstrahlung absorption, corrected for stimulated emission,

$$\sigma(v, T, x) = \gamma(x) \frac{1 - e^{-hv/kT}}{(hv)^3},$$

where

$$\gamma(x) = \begin{cases} 1 \text{ keV}^3/\text{cm}, & 0 < x < 1, \\ 1000 \text{ keV}^3/\text{cm}, & 1 < x < 2, \\ 1 \text{ keV}^3/\text{cm}, & 2 < x < 4. \end{cases}$$

We define $\sigma_g(T)$ to be the group average of the above formula at the zone centers;

$$\sigma_g(T) \equiv \frac{1}{v_{g+\frac{1}{2}} - v_{g-\frac{1}{2}}} \int_{v_{g-\frac{1}{2}}}^{v_{g+\frac{1}{2}}} \sigma(v, T, x_i) dv.$$

The heat capacity C_p is the constant $5.109 \times 10^{14} \text{ erg keV}^{-1} \text{ cm}^{-3}$.

We complete the introduction of Larsen’s test problem with a description of the problem’s energy sources. The initial temperature is $T(x, 0) = 10^{-3} \text{ keV}$, which is in equilibrium with the initial intensity $\psi_{g,d}(x, 0) = B_g(T(x, 0))$. No photons enters from the left boundary, but a steady, direction independent, 1 keV Planckian distribution of photons, $\psi_{g,d}(4 \text{ cm}, t) = B_g(1 \text{ keV})$, enters from the right boundary. The external heat source, q , and the external photon source, $s_{g,d}$, are both zero.

Turning to mathematics, the theorem of [5] sets an upper bound and a lower bound for the temperature of this problem. The upper bound is the largest temperature amongst the temperatures which specify the initial conditions and the boundary conditions of this problem. These temperatures are the initial material temperature $T(x, 0) = 10^{-3} \text{ keV}$, the temperature of the Planckian distribution of the initial intensity $\psi_{g,d}(x, 0) = B_g(T(x, 0))$, the temperature of the Planckian distribution of photons on the right inflow boundary $\psi_{g,d}(4 \text{ cm}, t) = B_g(1 \text{ keV})$, and the temperature of 0 keV that characterizes the empty Planckian on the left inflow boundary. The lower bound of the theorem is the smallest of these temperatures. The temperature of this problem is therefore

$$0 \text{ keV} \leq T(x, t) \leq 1 \text{ keV}. \tag{4.1}$$

The robustness of a method can be defined by its ability to yield a solution that is within these limits. Let us look at the robustness of the SiL and the PFM methods. Since the exact solution of this problem is unknown, we define the ‘exact’ solution to be the solution, which is computed by the fully implicit PFM method on the fine phase space grid, that has 2 times more spatial zones and 30 times smaller time steps than the phase space grid, described in the beginning of this section. At the time of 600 ps, we plot in Fig. 1 the ‘exact’ solution, the SiL solution, and the PFM solution. Both approximate solutions are, within discretization error, in agreement with the ‘exact’ solution, and both are also within the bounds of (4.1). It took 54 s of computer time to compute the SiL solution, and 110 s of computer time to compute the PFM solution.

Now let us look at the results as the time step is increased to 100 ps, 300 ps, and 600 ps. The SiL solutions, computed with the time steps of 30, 100, and 300 ps, are plotted on the l.h.s. of Fig. 2. In the 100 ps time step solution, although a slight oscillation appears at a point near $x = 1.8 \text{ cm}$, this solution is within the bounds of (4.1). However, the 300 ps time step solution is negative and is outside the limits of (4.1). The 600 ps time step solution is not plotted in Fig. 2, because it is not within the scale of the figure; the peak temperature of the 600 ps time step solution is more than 18 times larger than the peak temperature of the 30 ps time step solution. Let us turn to the results by the PFM method, which are plotted on the r.h.s. of Fig. 2. The PFM results are smoother than and more accurate than the SiL results.

The PFM method is more selective of a solution than the SiL method, because the PFM method screens a solution with more accuracy tests than the SiL method. The difference making test, not in the SiL method’s battery of tests, is administered at the outer step of Newton’s method. In this step, Newton’s method accepts an iterate only if the nonlinear residual of the iterate is smaller than a prescribed tolerance. On the other hand, the SiL method accepts a solution, which is untested by the nonlinear residual, $\mathcal{G}(\psi, T)$ of (2.2), from which the SiL equations are derived. The nonlinear residual is thus the gate-keeper in Newton’s method; it guards against inaccurate solutions.

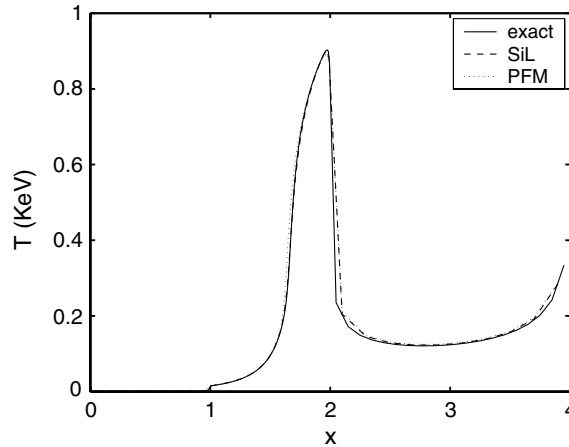


Fig. 1. The PFM and the SiL solutions compared to a reference solution at $t = 600$ ps.

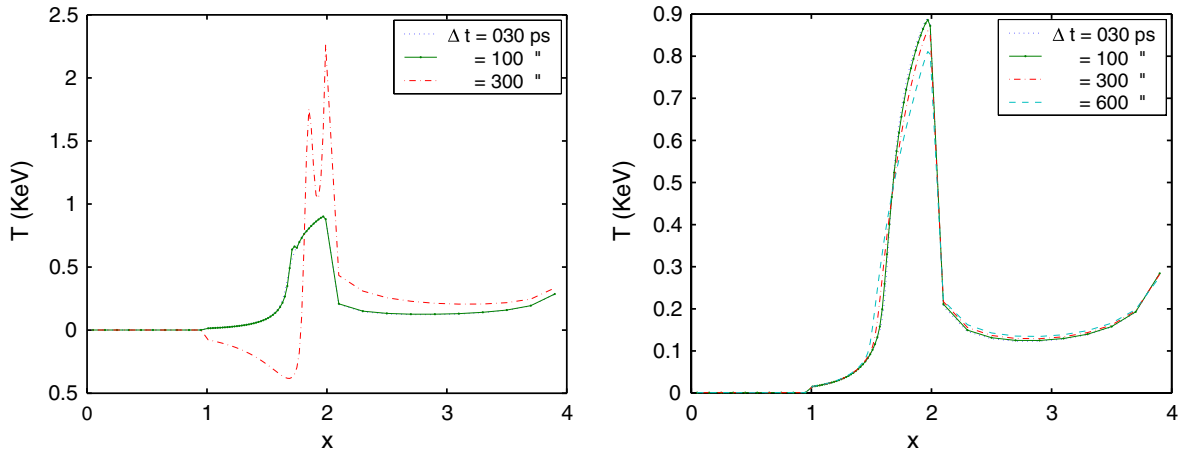


Fig. 2. SiL results are on the left, and PFM results are on the right.

However, this safeguard comes with a price; the cost to compute the nonlinear residual and its norm. Although this cost is a fixed overhead in Newton's method, we can minimize the total cost of Newton's method by lowering the cost of the linear update in Newton's method with effective preconditioning of the Jacobian. Let's examine the third row in the upper half of [Table 1](#) which shows the accelerating effect of the heat conducting preconditioner. Each entry in the first three rows of the table contains two numbers; the number to the left of the colon is a PFM result computed without preconditioning, and the number to the right of the colon is the PFM result computed with preconditioning. Let us look at the worst case first, the 600 ps time step solution. This case, performed in 1 time step, required 161 GMRES iterations, but only 123 preconditioned GMRES iterations to be carried out. The effectiveness of the heat conducting preconditioner improves dramatically with decreasing time step. In the calculations taken with 300 ps, 100 ps, and 30 ps time steps, GMRES need 50% fewer iterations to invert the Jacobian with preconditioning than without.

Now let us compare the run times of the two methods. The PFM method is clearly slower than the SiL method for this problem, because the PFM method has more chores to do than the SiL method. The extra tasks are: (1) to keep the coefficients $C_p(T)$ and $\sigma_g(T)$ current at temperature T , (2) to keep the Planckian $B_g(T)$ also current at temperature T , and (3) to compute the nonlinear residual and its norm. If the coefficients are weak functions of temperature, as they are in this problem [18], then keeping them current with costly

Table 1
Iteration statistics of calculations for different time steps

	Δt	30 (ps)	100 (ps)	300 (ps)	600 (ps)
PFM	Runtime (s)	123:110	118:81	157:116	175:155
	Nonlinear iterations	24:24	20:20	15:15	13:12
	Total linear iterations	49:24	76:30	126:61	161:123
SIL	Run time	54	24	7	2

The calculations, labeled by time step, are ordered by columns. The rows are the first is the total run times of the calculations, the second is the total number of nonlinear iterations taken by Newton’s method, and the third is the total number of linear iterations taken by GMRES. Each entry in the first three rows of the table contains two numbers: the number to the left of the colon is a result without preconditioning, and the number to the right of the colon is the result with preconditioning.

function evaluations is overkill. However, we cannot cut corners with the Planckian, because its nonlinearity is an essential characteristic of (2.2). The nonlinear residual is also essential in Newton’s method for two reasons: it is the r.h.s. of the linear update, and it is the metric by which we measure the accuracy of the PFM solution. The cost to compute the nonlinear residual, which enables us to control the accuracy of the PFM solution, is high, but is an expenditure that is well worth its cost.

4.2. The Problem of Su and Olson

The nonlinear system, solved analytically by Su and Olson [31], is the frequency integrated transport equation,

$$\left(\frac{1}{c} \frac{\partial}{\partial t} + \mu \frac{\partial}{\partial x} + \sigma\right) I(\mu, x, t) = \frac{1}{2} \sigma acT^4 + \frac{1}{2} acH\left(x - \frac{1}{2}\right)H\left(\frac{1}{2} - x\right)H\left(\frac{10}{c} - t\right),$$

and the material equation,

$$4aT^3 \frac{\partial T}{\partial t} = \int_{-1}^1 \sigma \left(I(\mu, x, t) - \frac{1}{2} acT^4 \right) d\mu,$$

where H is the Heaviside function, a is the radiation constant, c is the speed of light, and

$$I(\mu, x, t) \equiv \int_0^\infty \psi(v, \mu, x, t) dv.$$

The initial conditions are $T(x, 0) = 0$ and $I(\mu, x, 0) = 0$, and the boundary conditions are $\lim_{x \rightarrow \pm\infty} I(\mu, x, t) = 0$.

We simulate this problem as follows: the angular integral is approximated by the 20 point Gauss-Legendre quadrature. Since the problem is reflection symmetric, we solve the problem in the half space with the spatial grid,

$$\Delta x = \begin{cases} .020, & .0 < x < .1, \\ .100, & .1 < x < .5, \\ .125, & .5 < x < 1, \\ 1.00, & 1. < x < 35. \end{cases}$$

In the half space, no photons enters from the right boundary, and photons are reflected at the left boundary. The spatial derivative is approximated by the simple corner balance method [1]. Since the PFM and the SiL methods both cannot handle the singular perturbation caused by a vanishing heat capacity which occurs when the temperature is 0, we modify the initial temperature to be .001 everywhere.

The spatial profiles of the fourth power of the material temperature, computed by the PFM method at 3 time points, are plotted on the l.h.s. of Fig. 3. The time points are .1, 1, and 10 in the units in which the speed of light is 1. At these time points, we also plot the spatial profiles of the photon’s energy density on the r.h.s. of Fig. 3. The profiles were calculated with a constant time step of .1/20, the largest time step with which we

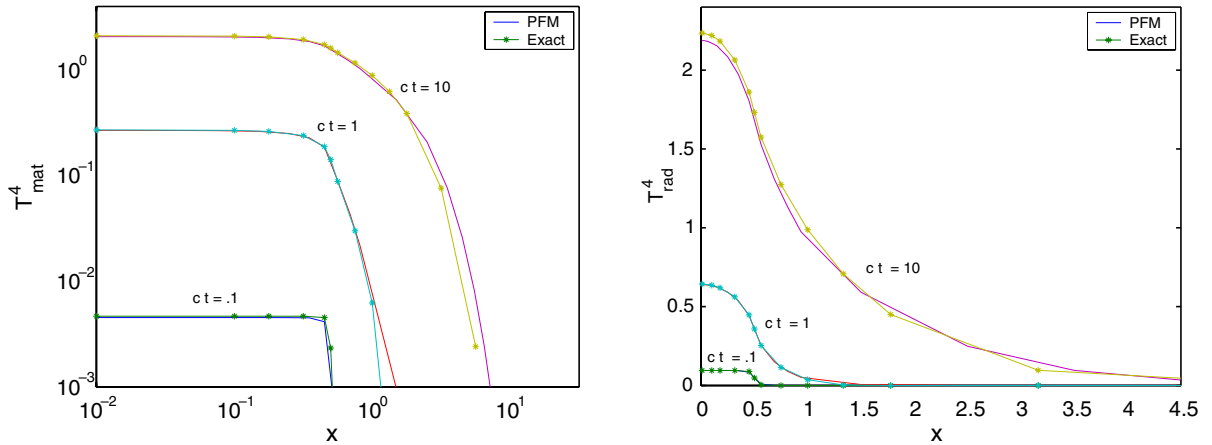


Fig. 3. The fourth power of the material temperature is on the left, and radiation energy density is on the right. It took the PFM method less than 10 s of computer time to evolve the solution to the time point $ct = .1$ with a time step of $c\Delta t = .1/20$.

found reasonable agreement between them and the analytical solution. It took less than 10 s of computer time to evolve the PFM solution to the first time point.

However, in order to calculate a solution of comparable accuracy, the SiL method requires a 200 times smaller time step than the PFM method. As a consequence of the smaller time step, the SiL method needs 49 times more computer time to solve this problem than the PFM method. The SiL solution at time $ct = .1$, which is plotted in Fig. 4, is less accurate than the PFM solution of the preceding figure. These results show that the linearizing approximation and the lagging approximation of the SiL method are damaging simplifications for this problem. However, the approximations of the SiL method, which were developed to deal with the nonlinearities of radiation equations, are unnecessary for solving the equations of Su and Olson, because the equations of Su and Olson are linear in the variables I and T^4 , and have constant coefficients.

We transform the equations of Su and Olson to these variables, and solve the transformed system by the SiL method⁶ with a time step of $c\Delta t = .1/20$, the time step by which the PFM solution plotted in the previous figure is evolved, and with the initial condition $T^4(x, t = 0) = 10^{-6}$. The results of the transformed system, labeled as T^4 in Fig. 4, are comparable in accuracy to the PFM solution of the previous figure, and to the SiL results of the untransformed system plotted in this figure. It also took the SiL method half as much time to solve the transformed equations as it took the PFM method to solve the untransformed equations. The SiL method performs better on the transformed equations than on the untransformed equations, because the set of transformed equations is a linear system but the set of untransformed equations is not. In conclusion, the tests in this section and in the previous section show that the lagging approximation and the linearizing approximation of the SiL method are simplifications which limit the time step that the SiL method can take accurately.

5. Discussion

5.1. A comparison with the SiL approximation

In order to compare the PFM with conventional deterministic radiative transfer methods [3,18,26,28], we shall derive the SiL equations which are solved by them. For the reader's convenience, we move (2.2), the system solved by the PFM, into (5.1) of this section

$$\begin{aligned}
 (\mu_d D + \sigma_g(T) + (c\Delta t_n)^{-1} I) \psi_{g,d} &= \sigma_g(T) B_g(T) + s_{g,d} + (c\Delta t_n)^{-1} \psi_{g,d}^n + b_{g,d}, \\
 C_p(T) \frac{T - T^n}{\Delta t_n} &= \sum_{g=1}^{n_g} \sum_{d=1}^{n_d} \sigma_g(T) w_d (\psi_{g,d} - B_g(T)) + q.
 \end{aligned} \tag{5.1}$$

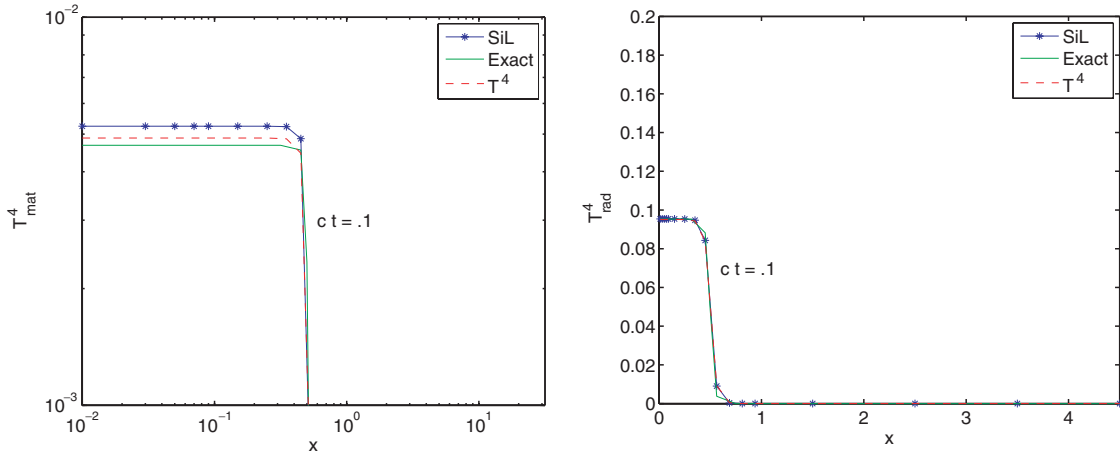


Fig. 4. The fourth power of the material temperature is on the left, and radiation energy density is on the right. It took the SiL method 494 s of computer time to obtain the solution at $ct = .1$ with a time step of $c\Delta t = .1/4000$. The solution, labeled by T^4 , is the result of solving the system expressed in terms of the variables I and T^4 .

While it is easy to eliminate $\psi_{g,d}$ from (5.1) since (5.1) is linear in $\psi_{g,d}$, it is difficult to eliminate T from (5.1) since (5.1) is nonlinear in T . In order to analytically eliminate T from (5.1), the SiL approximation makes two approximations: it freezes the coefficients of (5.1) to their values at the beginning of the time step, and it approximates the black body emission function with a linear function of temperature that is centered about the beginning of the time step. We denote the frozen coefficients as

$$\sigma_g^n \equiv \sigma_g(T^n), \quad \text{and} \quad C_p^n \equiv C_p(T^n), \tag{5.2}$$

and we denote the SiL’s linear model for the black body function as

$$B_g(T) \approx B_g^n + \dot{B}_g^n(T - T^n), \quad \text{where} \quad B_g^n \equiv B_g(T^n), \quad \text{and} \quad \dot{B}_g^n \equiv \left. \frac{dB_g}{dT} \right|_{T^n}. \tag{5.3}$$

The substitution of (5.2) and (5.3) into (5.1) yields

$$\begin{aligned} (\mu_d D + \sigma_g^n + (c\Delta t_n)^{-1} I) \psi_{g,d}^{SiL} &= \sigma_g^n (B_g^n + \dot{B}_g^n (T - T^n)) + s_{g,d} + (c\Delta t_n)^{-1} \psi_{g,d}^n + b_{g,d}, \\ C_p^n \frac{T - T^n}{\Delta t_n} &= \sum_{g=1}^{n_g} \sum_{d=1}^{n_d} \sigma_g^n w_d (\psi_{g,d}^{SiL} - (B_g^n + \dot{B}_g^n (T - T^n))) + q. \end{aligned} \tag{5.4}$$

Since (5.4) is a linear system, we can solve the second equation of (5.4) for $T - T^n$ and substitute the result into the first equation of (5.4) to give the Schur complement of (5.4), which is the transport-like equation of the SiL approximation of (5.1),

$$\begin{aligned} (\mu_d D + \sigma_g^n + (c\Delta t_n)^{-1} I) \psi_{g,d}^{SiL} &= \alpha_g^n \sum_{g'=1}^{n_g} \sum_{d'=1}^{n_d} \sigma_{g'}^n w_{d'} \psi_{g',d'}^{SiL} - \alpha_g^n \sum_{g'=1}^{n_g} \sum_{d'=1}^{n_d} \sigma_{g'}^n w_{d'} B_{g'}^n + \alpha_g^n q + \sigma_g^n B_g^n + s_{g,d} \\ &\quad + (c\Delta t_n)^{-1} \psi_{g,d}^n + b_{g,d}, \end{aligned} \tag{5.5}$$

where

$$\alpha_g^n \equiv \frac{\sigma_g^n \dot{B}_g^n}{\frac{C_p^n}{\Delta t_n} + \sum_{g'=1}^{n_g} \sum_{d'=1}^{n_d} \sigma_{g'}^n w_{d'} \dot{B}_{g'}^n}.$$

Conventional deterministic simulations [3,18,26,28] of continuum radiative transfer are obtained not by solving (5.1) but by solving (5.4)⁷.

6. Summary

In this paper, we showed that the solution to the equations of continuum radiation transport can be found by searching in a space of much lower dimensionality than the space of the underlying transport equations. The lower dimensional object of this search is the temperature, and is determined by a material-like equation, which is derived by the elimination of the intensity variable from the primal system. The reduced system of equations has the form of a nonlinear integral equation in which a nonlinear heat equation is buried. A preconditioner to accelerate the inversion of the Jacobian of the reduced system is derived from the nonlinear heat equation. The PFM method is the first method to solve the nonlinear equations of continuum radiation transport with unfrozen coefficients. It is also the first method to solve the radiation equations through a subsidiary set of equations which is free of photon variables.

Acknowledgements

I thank S. Lee and P. N. Brown for bringing me up to speed on nonlinear methods. I also thank John Castor for our discussions on radiation transport. This work was performed under the auspices of the US Department of Energy by Lawrence Livermore National Laboratory Under Contract No. W-7405-Eng-48. UCRL-JRNL-218676.

Appendix 1. A Matrix-free Jacobian-vector product

In this section, we drop the subscript k for the current iterate. A convenient starting point for the derivation of the Jacobian of $\mathcal{F}(T)$ is the system

$$\begin{aligned} \mathcal{F}(T) &= C_p(T)(T - T^n) - \sum_{g,d=1}^{n_g, n_d} \Delta t_n \sigma_g(T) w_d (\psi_{g,d}(T) - B_g(T)) - q \Delta t_n, \\ H_{g,d}(T) \psi_{g,d}(T) &= \sigma_g(T) B_g(T) + f_{g,d}^n, \end{aligned} \quad (7.1)$$

where the second equation is (2.6). Differentiating the first equation of (7.1) gives

$$\begin{aligned} \frac{\partial \mathcal{F}}{\partial T} &= \frac{\partial(C_p(T)(T - T^n))}{\partial T} - \sum_{g,d=1}^{n_g, n_d} \Delta t_n \frac{\partial \sigma_g(T)}{\partial T} w_d (\psi_{g,d}(T) - B_g(T)) \\ &\quad - \sum_{g,d=1}^{n_g, n_d} \Delta t_n \sigma_g(T) w_d \left(\frac{\partial \psi_{g,d}(T)}{\partial T} - \frac{\partial B_g(T)}{\partial T} \right). \end{aligned}$$

It is straightforward to determine the partial derivatives of $C_p(T)$, $\sigma_g(T)$, and $B_g(T)$, because each component of these functions is a function of a single variable. On the other hand, it is more involved to determine the partial derivative of $\psi_{g,d}(T)$. Differentiating the second equation of (7.1) and solving the resulting equation for $\partial \psi_{g,d}(T) / \partial T$, gives

$$\frac{\partial \psi_{g,d}(T)}{\partial T} = H_{g,d}^{-1} \left(\frac{\partial(\sigma_g(T) B_g(T))}{\partial T} - \frac{\partial H_{g,d}(T)}{\partial T} \psi_{g,d}(T) \right). \quad (7.2)$$

The calculation of $\partial \mathcal{F}(T) / \partial T$ requires the solutions of two transport equations. The first is to determine $\psi_{g,d}$ and the second is to determine $\partial \psi_{g,d}(T) / \partial T$.

Since the Jacobian is a dense $n_x \times n_x$ matrix, where n_x is the number of zones, then forming the Jacobian in a simulation would be, because of its size, impractical for large scale simulations. Fortunately, the GMRES

⁷ Methods [3] and [28] solve a simplification of (5.1) by iteration with an equation of the form of (5.4); their simulations are, however, restricted to frozen coefficients.

method requires only the action of the Jacobian on an arbitrary, say z . The rest of this Appendix is devoted to the derivation of a matrix-free formula for computing $\mathbf{J}z$.

We introduce notation for the components of the functions $C_p(T)$, $\sigma_g(T)$ and $B_g(T)$ to facilitate the derivation. Each component of the diagonal matrix, $C_p(T)$, for example, is a function of a single temperature. If $(C_p(T))_i$ is the heat capacity of zone i , then it is a function of T_i , the temperature of zone i , and independent of the temperature elsewhere. Therefore, we label the heat capacity of zone i by T_i , we write

$$(C_p(T))_i \equiv C_p(T_i), \quad \text{the heat capacity of zone } i.$$

Furthermore, the Jacobian of $C_p(T)$ is the diagonal matrix

$$\left(\frac{\partial C_p(T)}{\partial T}\right)_{i,j} \equiv \frac{\partial (C_p(T))_i}{\partial T_j} = \begin{cases} \frac{\partial C_p(T_i)}{\partial T_i}, & i = j \\ 0, & i \neq j \end{cases}.$$

Similarly, since each component of $\sigma_g(T)$ and of $B_g(T)$, is a function of a single temperature, the Jacobians of $\sigma_g(T)$ and of $B_g(T)$ are also diagonal matrices.

Component i of $\mathbf{J}z$ can be written as:

$$\begin{aligned} (\mathbf{J}z)_i &= \sum_{j=1}^{n_x} \frac{\partial (C_p(T_i)(T_i - T_i^n))}{\partial T_j} z_j - \sum_{g,d,j=1}^{n_g, n_d, n_x} \Delta t_n w_d (\psi_{i,g,d} - B_g(T_i)) \frac{\partial \sigma_g(T_i)}{\partial T_j} z_j \\ &\quad - \sum_{g,d,j=1}^{n_g, n_d, n_x} \Delta t_n \sigma_g(T_i) w_d \left(\frac{\partial \psi_{i,g,d}}{\partial T_j} - \frac{\partial B_g(T_i)}{\partial T_j} \right) z_j. \end{aligned}$$

Since the Jacobians of $C_p(T)$, $\sigma_g(T)$ and $B_g(T)$ are diagonal matrices, then the sums with respect to j , which involve these Jacobians and the vector z , collapse to a single term. Collapsing these sums in the above equation, we have, after minor rearrangement,

$$\begin{aligned} (\mathbf{J}z)_i &= \frac{\partial (C_p(T_i)(T_i - T_i^n))}{\partial T_i} z_i - \sum_{g,d=1}^{n_g, n_d} \Delta t_n w_d (\psi_{i,g,d} - B_g(T_i)) \frac{\partial \sigma_g(T_i)}{\partial T_i} z_i + \sum_{g,d=1}^{n_g, n_d} \Delta t_n \sigma_g(T_i) w_d \frac{\partial B_g(T_i)}{\partial T_i} z_i \\ &\quad - \sum_{g,d,j=1}^{n_g, n_d, n_x} \Delta t_n \sigma_g(T_i) w_d \frac{\partial \psi_{i,g,d}}{\partial T_j} z_j. \end{aligned}$$

It is straightforward to calculate the first three terms on the r.h.s. of the above equation. The sum with respect to j in the last term of the above equation can be simplified. Substituting the r.h.s. of (7.2) for $\partial \psi_{i,g,d} / \partial T_j$, we have for this sum

$$\sum_{j=1}^{n_x} \frac{\partial \psi_{i,g,d}}{\partial T_j} z_j = \sum_{j,k=1}^{n_x, n_x} (H_{g,d}^{-1})_{i,k} \left(\frac{\partial (\sigma_g(T_k) B_g(T_k))}{\partial T_k} z_j - \sum_{l=1}^{n_x} \frac{\partial (H_{g,d}(T))_{k,l}}{\partial T_k} \psi_{l,g,d} z_j \right). \quad (7.3)$$

With the exception of the partial derivatives of $H_{g,d}(T)$, the formulas for the other terms on the r.h.s. have been given already. Referring to (2.3), the elements of $H_{g,d}(T)$, with the aid of the Kronecker delta, can be written as $(H_{g,d}(T))_{k,l} = \mu_d D_{k,l} + \sigma_g(T_k) \delta_{k,l} + (c \Delta t_n)^{-1} \delta_{k,l}$. Thus, we have

$$\frac{\partial (H_{g,d}(T))_{k,l}}{\partial T_j} = \frac{\partial \sigma(T_k)}{\partial T_j} \delta_{k,l} \delta_{k,j} = \frac{\partial \sigma_g(T_k)}{\partial T_k} \delta_{k,j} \delta_{k,l} \delta_{k,j}.$$

The last equality follows because $\partial \sigma_g(T_k) / \partial T_j$ is zero unless $k = j$. Using this result and the diagonality of the Jacobians of $\sigma_g(T)$ and $B_g(T)$, the sums with respect to j and l on the r.h.s. (7.3) reduce to

$$\sum_{j=1}^{n_x} \frac{\partial \psi_{i,g,d}}{\partial T_j} z_j = \sum_{k=1}^{n_x} (H_{g,d}^{-1})_{i,k} \left(\frac{\partial (\sigma_g(T_k) B_g(T_k))}{\partial T_k} z_k - \frac{\partial \sigma_g(T_k)}{\partial T_k} z_k \psi_{k,g,d} \right).$$

The above equation is a matrix-free formula for the action the Jacobian of $\psi_{g,d}$ on the vector z . It computed by forming the source term, $\frac{\partial (\sigma_g(T_k) B_g(T_k))}{\partial T_k} z_k - \frac{\partial \sigma_g(T_k)}{\partial T_k} z_k \psi_{k,g,d}$, and then following it up with a sweep by $H_{g,d}^{-1}$.

Collecting terms, the matrix-free formula for computing the action of $\partial \mathcal{F} / \partial T$ on the vector z is

$$(\mathbf{J}z)_i = \frac{\partial(C_p(T_i)(T_i - T_i^n))}{\partial T_i} z_i + \sum_{g,d=1}^{n_g n_d} \Delta t_n \sigma_g(T_i) w_d \frac{\partial B_g(T_i)}{\partial T_i} z_i - \sum_{g,d=1}^{n_g n_d} \Delta t_n w_d \frac{\partial \sigma_g(T_i)}{\partial T_i} z_i (\psi_{i,g,d}(T) - B_g(T_i)) - \sum_{g,d,k=1}^{n_g n_d n_x} \Delta t_n \sigma_g(T_i) w_d \left(H_{g,d}^{-1} \right)_{i,k} \left(\frac{\partial(\sigma_g(T_k) B_g(T_k))}{\partial T_k} z_k - \frac{\partial \sigma_g(T_k)}{\partial T_k} z_k \psi_{k,g,d} \right),$$

where $\psi_{g,d}(T)$ is determined by solving (2.6). This formula requires two sweeps for each group and each direction; the first is to get $\psi_{g,d}(T)$ and the second is to compute the last term in the formula.

Appendix 2. An initial guess for solving $\mathcal{F}(T) = 0$ by Newton's method

The efficiency of Newton's method can be improved with an initial guess which is close to the root of $\mathcal{F}(T)$. When the time step is large, the temperature at the old time step, T^n , can be far from the root of $\mathcal{F}(T)$. However, we found that an initial guess, which is closer to T than T^n , can be obtained from an approximation of $\mathcal{F}(T)$ which is easy to solve. To derive that approximation, we return to (2.2) and observe that D is a non-diagonal matrix (and is the only non-diagonal matrix in the system of equations), which makes, $\mathcal{F}(T) = 0$, difficult to solve. Approximating $D\psi_{g,d}$ by $D\psi_{g,d}^n$, and putting $D\psi_{g,d}^n$ on the r.h.s. of (2.2), the non-diagonality of D is rendered a non-issue; another approximation for D is its diagonal. If $H_{a,g,d}(T_0)$ is the diagonal matrix,

$$H_{a,g,d}(T_0) \equiv \sigma_g(T_0) + (c\Delta t_n)^{-1} I,$$

and $f_{a,g,d}^n$ is the modified source term,

$$f_{a,g,d}^n \equiv s_{g,d} + (c\Delta t_n)^{-1} \psi_{g,d}^n + b_{g,d} - \mu_d D\psi_{g,d}^n,$$

of the transport equation for that approximation, then $\mathcal{F}_a(T_0)$, the approximation of $\mathcal{F}(T)$ for T_0 , can be written as:

$$\mathcal{F}_a(T_0) \equiv C_p(T_0)(T_0 - T^n) - q\Delta t_n - \sum_{g,d=1}^{n_g n_d} \Delta t_n \sigma_g(T_0) w_d (H_{a,g,d}^{-1}(T_0) (\sigma_g(T_0) B_g(T_0) + f_{a,g,d}^n) - B_g(T_0)).$$

It is easy to solve $\mathcal{F}(T_0) = 0$, because $\mathcal{F}_a(T_0) = 0$ is a set of single variable functions. The zero of a nonlinear function of a single variable can be found easily by a multitude of failsafe methods, e.g. regula falsi, secant, etc.

References

- [1] M.L. Adams, Sub-cell balance methods for radiative transfer on arbitrary grids, *Transp. Theory Stat. Phys.* 26 (1997) 385–431.
- [2] M.L. Adams, E.W. Larsen, Fast iterative methods for discrete-ordinates particle transport calculations, *Prog. Nucl. Energy* 40 (1) (2002) 3–159.
- [3] M.L. Adams, P. Nowak, Asymptotic analysis of a computational method for time and frequency-dependent radiation transfer, *J. Comp. Phys.* 146 (1998) 366–403.
- [4] R.E. Alcouffe, Diffusion synthetic acceleration methods for the diamond-difference discrete-ordinates equations, *Nucl. Sci. Eng.* 64 (1977) 344–355.
- [5] E.S. Amdreev, M.Yu. Kozmanov, E.B. Rachilov, The maximum principle for a system of equations of energy and non-stationary radiation transfer, *USSR Comput. Math. Math. Phys.* 23 (1) (1983) 104–109.
- [6] Y.Y. Azmy, The weighted diamond-difference form of nodal transport methods, *Nucl. Sci. Eng.* 98 (1988) 29–40.
- [7] E.D. Brooks, Symbolic implicit Monte Carlo, *J. Comp. Phys.* 83 (2) (1989) 433–446.
- [8] P.N. Brown, A linear algebraic development of diffusion synthetic acceleration for three-dimensional transport equations, *Siam J. Numer. Anal.* 32 (1) (1995) 179–214.
- [9] P.N. Brown, Y. Saad, Hybrid Krylov methods for nonlinear systems of equations, *SIAM J. Sci. Statist. Comput.* 11 (3) (1990) 450–481.
- [10] P.N. Brown, D.E. Shumaker, C.S. Woodward, Fully implicit solution of large-scale non-equilibrium radiation diffusion with higher order time integration, *J. Comp. Phys.* 204 (2005) 760–783.
- [11] B.G. Carlson, K.D. Lathrop, Transport theory the method of discrete ordinates, in: H. Greenspan, C.N. Kelber, D. Okrent (Eds.), *Computing Methods in Reactor Physics*, Gordon and Breach, New York, 1968, pp. 167–266.
- [12] A.S. Eddington, *Mon. Not. R. Astr. Soc.* 77 (1916) 16.

- [13] A.M. Collier, A.C. Hindmarsh, R. Serban, C.S. Woodward, User Documentation for KINSOL v2.3.0, Lawrence Livermore National Lab, UCRL-SM-208116.
- [14] J.A. Fleck Jr., J.D. Cummings, An implicit Monte Carlo scheme for calculating time and frequency dependent nonlinear radiation transport, *J. Comp. Phys.* 8 (1971) 315–342.
- [15] A. Greenbaum, J.M. Ferguson, A Petrov–Galerkin finite element for solving the neutron transport equation, *J. Comp. Phys.* 64 (1986) 97–111.
- [16] C.T. Kelley, Solving nonlinear equations with newton’s method, *Fundamentals of Algorithms Series*, SIAM, 2003.
- [17] E.W. Larsen, Unconditionally stable diffusion-synthetic acceleration methods for the slab geometry discrete ordinates equations. Part I: theory, *Nucl. Sci. Eng.* 82 (1982) 47–63.
- [18] E.W. Larsen, A grey transport acceleration method for time-dependent radiative transfer problems, *J. Comp. Phys.* 78 (2) (1988) 459–480.
- [19] E.W. Larsen, B. Mercier, Analysis of a Monte Carlo method for nonlinear radiative transfer, *J. Comp. Phys.* 71 (1987) 50–64.
- [20] E.W. Larsen, G.C. Pomeraning, V.C. Badham, Asymptotic analysis of radiative transfer problems, *J. Quant. Spectrosc. Radiat. Transfer.* 29 (4) (1981) 285–310.
- [21] R.B. Lowrie, A comparison of implicit time integration methods for nonlinear relaxation and diffusion, *J. Comp. Phys.* 196 (2004) 566–590.
- [22] R.E. Marshak, Effect of radiation on shock wave behavior, *Phys. Fluids* 1 (1) (1958) 24–29.
- [23] V.A. Mousseau, D.A. Knoll, New physics-based preconditioning of implicit methods for non-equilibrium radiation diffusion, *J. Comp. Phys.* 190 (2003) 42–51.
- [24] D.R. McCoy, E.W. Larsen, Unconditionally stable diffusion-synthetic acceleration methods for the slab geometry discrete ordinates equations. Part II: numerical results, *Nucl. Sci. Eng.* 82 (1982) 47–63.
- [25] M.S. McKinley, E.D. Brooks, A. Szoke, Comparison of implicit and symbolic implicit Monte Carlo line transport with frequency weight vector extension, *J. Comp. Phys.* 189 (1) (2003) 330–349.
- [26] J.E. Morel, T.A. Wareing, K. Smith, A linear-discontinuous spatial difference scheme for Sn radiative transfer calculations, *J. Comp. Phys.* 128 (1996) 445–462.
- [27] T. N’Kaoua, Solution of the nonlinear radiative transfer equations by a fully implicit matrix Monte-Carlo method coupled with the rosseland diffusion equation via domain decomposition, *SIAM J. Sci. Stat. Comput.* 12 (3) (1991) 505–520.
- [28] P.F. Nowak, M. Nemanic, Radiation Transport Calculations on Unstructured Grids using a Spatial Decomposed and Threaded Algorithm, Lawrence Livermore National Lab, UCRL- JC-133787.
- [29] W.H. Reed, T.R. Hill, *Triangular Mesh Methods for the Neutron Transport Equation*, LA-UR-73-479, Los Alamos National Laboratory, 1973.
- [30] Y. Saad, *Iterative Methods for Sparse Linear Systems*, PWS Publ. Co., Boston, 1996.
- [31] B.J. Su, G.L. Olson, An analytic benchmark for nonequilibrium radiative transfer in an isotropically scattering medium, *Ann. Nucl. Energy* 24 (13) (1977) 1035–1055.